Study on structure characteristics of B_2O_3 and TiO_2-bearing F-free mold flux by Raman spectroscopy

Zhen WANG [1),2)], Qifeng SHU [1),2)] and Kuochih CHOU [1,2)]*

1) State Key Laboratory of Advanced Metallurgy, University of Science and Technology Beijing，Beijing 100083,China

2) School of Metallurgical and Ecological Engineering, University of Science and Technology Beijing, Beijng 100083, China

Abstract: Structure characteristics of fluoride-Free mold flux containing simultaneously B_2O_3 and TiO_2 have been investigated by Raman spectroscopy in this work. Raman spectra for glass samples with different basicities, different contents of TiO_2 and B_2O_3 were recorded during the experiments. According to the experiments results, increase of TiO_2 content leads to the appearance of $[TiO_4]$ and $[TiO_6]$ structure groups, and $[TiO_4]$ becomes the main structure unit in the system. TiO_2 produces a certain destructive effect on Si-O-Si network structure as well as large borate group and conducive to the formation of some other complex structure groups, such as (Si,Ti) coupling in sheet unit. It can be concluded that, with the increase of B_2O_3, the ratio of mixing of the Q^0 structure unit and $[TiO_4]$ structural group decrease and the ratio of sheet structure unit increase, and there forms large borate group. Existence of B_2O_3 increases polymerization degree of the slag system. In addition, increasing basicity causes to the decrease of Q^2 and sheet structure unit and increase of mixing of the Q^0 structure unit and $[TiO_4]$ structural group, and weakening the large borate group. It could be concluded that the increase of basicity reduces the degree of polymerization of the system.

Keywords: Fluoride-Free mold flux, B_2O_3 and TiO_2, structure, Raman spectroscopy

1. Introduction

As critical materials in continuous casting process, mold flux plays an irreplaceable role in metallurgical industry. However, the fluorides within traditional mold flux produce harmful influence both on the natural environment and on equipment seriously, such as, volatilization of fluorides leading to erosion to continuous caster, pollution of environment, acidification of the cooling water, human health hazard, and so on [1-4]. Thus, the development and application of fluorine free mould flux is of great significance and has become a research area of interest [2-5].It is reported that slags bearing B_2O_3 and /or TiO_2 become most promising substitute for traditional mould fluxes [2-8]. According to some previous studies [2, 4, 7, 8], the existence of TiO_2 in mould fluxes can easily lead to the formation of some crystals (eg. $CaTiO_3$ or $CaO\cdot SiO_2\cdot TiO_2$) with high melting point, which is potential to replace the cuspidine generated by fluorine in mould fluxes to ensure the crystallizability of slag to achieve good heat transfer performance. Besides, B_2O_3, as an effective fluxing agent to lower the melting point of mould flux, has been taken into consideration for being added to mould fluxes to adjust the viscosity or melting properties of slag [3, 5, 6].So it is absolutely essential to investigate the properties of mould fluxes simultaneously containing B_2O_3 and/or TiO_2 to develop the optimal fluorine free mould fluxes.

The performance of mold flux, such as heat transfer and lubricity, serves an important function to ensure the process stability of the continuous casting process and surface quality of products. And benign physio-chemical properties, which contribute the excellent performance of mold fluxes [1-9], are closely related to structure characteristic of slag. Knowledge of structure of molten slags is essential to understand the properties of slags. Consequently, it is practical importance of investigating the structure of mold slag to explore the appropriate physio-chemical properties of mold flux so as to guarantee the good performance, and thus achieve the purpose of controlling metallurgical processes.

For a better understanding of the structure characteristic of molten slag, a lot of analytical techniques have been developed and widely used, such as IR spectrum analysis, nuclear magnetic resonance (NMR), electronic probe rays microscopic analysis (EPMA), high temperature X-ray diffraction analysis, Raman spectroscopy, and so on. In comparison to other methods, Raman spectroscopy is with a lot of advantages in terms of microanalysis, high analysis speed, high precision and accuracy, application to high-temperature condition and no-destruction [10-14]. Therefore, Raman spectroscopy has been successfully applied to detect the vibration mode of molecular or micro-structure units and has become a very popular technique to acquire the information of constitutes and structure of materials [10-12].

It is effective to study the structure of high temperature melts through analyzing the Raman spectra of the corresponding glasses at room temperature in the fact that the spectra of glass and melts are similar based on the comparison of the infrared and Raman spectra of various silicate glasses and that of the corresponding melts by many researchers [13, 14]. Thus, the structure characteristic of B_2O_3 and TiO_2-bearing fluoride-free mold flux has been investigated by analyzing the room-temperature Raman spectra of the glass systems in this work. Structural information of glass systems with variable TiO_2 and B_2O_3 content and different basicities (R=w(CaO)/w(SiO_2)) were obtained by Raman spectra to examine the influences of TiO_2, B_2O_3 content and basicities on the structure of B_2O_3 and TiO_2-bearing fluoride-free mold flux.

2. Experimental

2.1 Sample preparation

Analytical grade CaO, SiO_2, Al_2O_3, MgO, TiO_2, Na_2CO_3 and H_3BO_3 were taken as raw materials, with Na_2CO_3 and H_3BO_3 being substitutes for Na_2O and B_2O_3, respectively. Table 1 presents the compositions (wt. %) of the glass samples investigated.

Glass samples with different TiO_2, B_2O_3 content and different basicities were prepared by the conventional melting and quenching method. Raw materials were mixed, taken into a platinum crucible and then melted in high temperature furnace at approximately 1573K in air atmosphere. The samples were held at 1573K for nearly 3h to make sure complete melting and homogenization. After melting, the melts were quenched by water and then bulk glass samples are formed. These glass samples are proved to be amorphous by XRD (e.g. Figure 1).

Table 1 Chemical compositions of experimental samples (wt. %)

Sample Number	basicity	CaO	SiO_2	Al_2O_3	MgO	Na_2O	TiO_2	B_2O_3
1	R=1	38	38	7	2	10	0	5
2		36.5	36.5	7	2	10	3	5
3		35.5	35.5	7	2	10	5	5
4		34.5	34.5	7	2	10	7	5
5		33	33	7	2	10	10	5
6		38	38	7	2	10	5	0
7		36.5	36.5	7	2	10	5	3
8		34.5	34.5	7	2	10	5	7
9		33	33	7	2	10	5	10
10	R=1.2	38.7	32.3	7	2	10	5	5
11	R=0.8	31.6	39.4	7	2	10	5	5

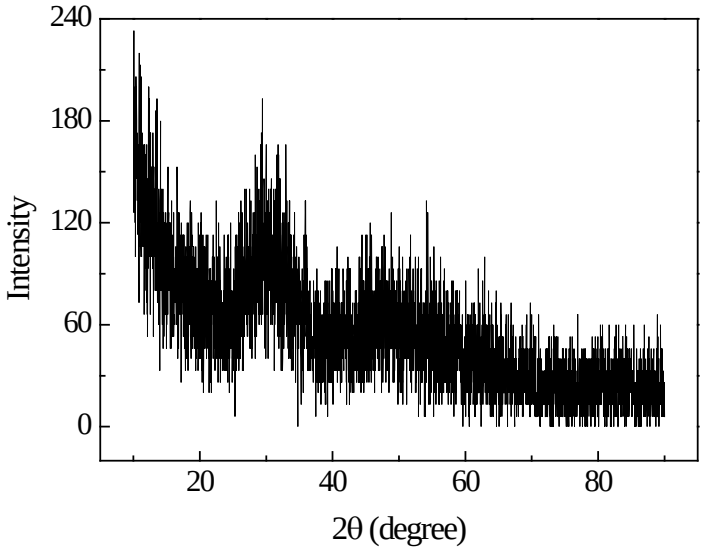

Fig. 1 A typical XRD pattern of the quenched sample

2.2 Raman spectroscopy measurement

Bulk glass samples were subjected to the Raman spectroscopy analysis. Raman spectra were acquired using a laser confocal micro-Raman spectrometer, JY-HR800, manufactured by Jobin Y'von of France. The experiments were carried out at room temperature using excitation wavelength of 532 nm and the light source was a semiconductor laser with power of 1mw. The frequency band measured in this work ranged from 100 to 2000 cm^{-1}.

3. Results and discussion

Figure 2, 3 and 4 present the room-temperature Raman spectra for glass samples with different contents of TiO_2, B_2O_3 and different basicities, respectively. All the backgrounds of the measured Raman signals have been subtracted. All of the measured Raman spectra of glass samples are deconvolved by Gaussian-Deconvolution method similar to method by Mysen et al. [15] with the minimum correlation coefficient $r^2 \geq 0.998$. The deconvoluted results have been shown in Figure 5, 7 and 9. The focus of attention in this work is the middle and high frequency of the Raman spectra. Assignments of Raman peaks that are to the interest of present work have been listed in Table 2.

Table 2 Assignments of Raman bands in spectra for the mold flux glass system

Raman shift (cm^{-1})	Raman assignments
677~680	O-Si-O deformation motion
690~700	Ti-O stretch vibrations of Ti in six-fold coordination ($[TiO_6]$)
~870	SiO_4^{4-} stretching in monomer structure unit (Q^0),or Q^4(4Al) structure unit
~950	SiO_3^{2-} stretching with two bridging oxygen in chain structure unit (Q^2)
1030~1037	Si-O^o antisymmetric stretching in any structural units that contain bridging oxygen
1192~1204	pyroborate group
1369~1379, 1435~1470	BO_2O^- triangles units attached to the large borate group

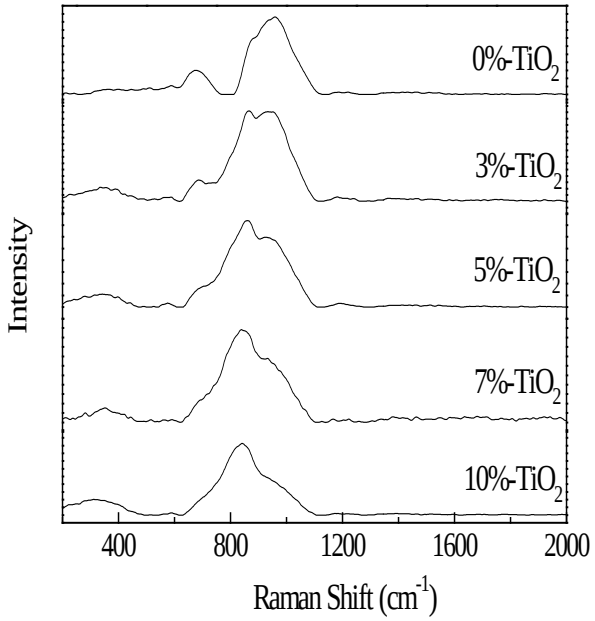

Fig. 2 Raman spectra for samples with different contents of TiO_2 (No. 1, 2, 3, 4 and 5) at room temperature, after background subtraction

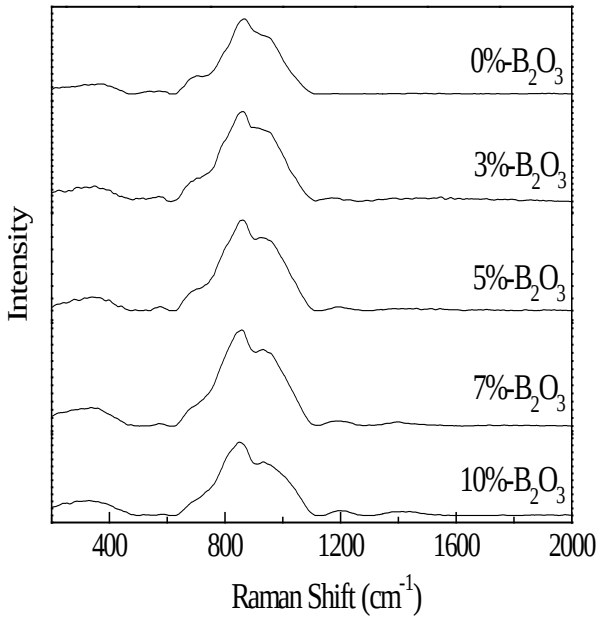

Fig. 3 Raman spectra for samples with different contents of B_2O_3 (No. 3, 6, 7, 8 and 9) at room temperature, after background subtraction

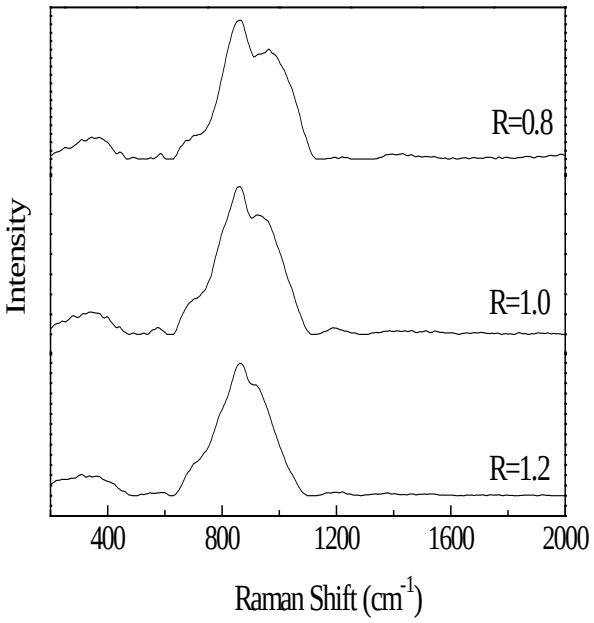

Fig. 4 Raman spectra for samples with different basicities (No. 3, 10 and 11) at room temperature, after background subtraction

Figure 5 shows the deconvoluted results of Raman spectra for glass systems with different TiO_2 content. It can be seen that in the TiO_2-free glass system (Figure 5 (a)), there is a dominant Raman peak at approximately 950 cm^{-1} which is due to SiO_3^{2-} stretching with NBO/Si=2 (non-bridging oxygen per tetrahedrally coordinated cation) and referred to as Q^2 (superscript refers to the number of bridging oxygen) species in a chain structure [16-21]. There are also three primary bands for sample without TiO_2, 679, ~870 and 1030 cm^{-1}. According to some previous researches [16-26], the band 679 cm^{-1} could be assigned to O-Si-O deformation motion, the 870 cm^{-1} band is assigned to SiO_4^{4-} stretching with NBO/Si=4 and referred to as Q^0 species in monomer structure, or it is due to Q^4(4Al) structure unit, and the band at about 1030 cm^{-1} is due to Si-O^o (O^o-bridging O atoms) antisymmetric stretching in any structural units that contain bridging oxygen but does not need be fully polymerized. It can be seen from Figure 5 that, as the addition of TiO_2 increases, the band at about 870 cm^{-1} becomes the dominant peak and simultaneously shifts toward low frequencies gradually, as 856, 840 and 838 cm^{-1}, the 1030 cm^{-1} band has shift toward low frequency, about 1012 and 997 cm^{-1} respectively, and the ~950 cm^{-1} peak shows a decrease in intensity. Based on the reports of Mysen et al [22, 27], for Ti-bearing silicate melts, the bands at about 830 and 810 cm^{-1} could correspond to the vibration of Si-O^{2-} structural unit and Ti-O^{2-} vibrations in the form of [TiO_4], respectively, so it can be presumed that the emerging bands with increase of TiO_2 content, 856, 840 and 838 cm^{-1} may indicate mixing of the Q^0 structure unit and [TiO_4] structural groups; the band in the range of 997~1030 cm^{-1} probably corresponds to the mixing of (Si,Ti) coupling of stretch vibrations in a sheet structure with randomly distribution of Ti^{4+} and Si^{4+} [22] and Si-O^o antisymmetric stretching in any structural units that contain bridging oxygen. Area ratios of the bands could reflect the abundance changes of different structure units, so the area fractions of bands in 600~1600 cm^{-1} are taken into consideration to descript the changes of structure groups in this work. Figure 6 presents the area fractions of bands in 600~1600 cm^{-1} as functions of TiO_2 contents. It can be seen that

with addition of TiO_2, the ratio of 838~875 cm^{-1} bands increases, the ratio of 944~966 cm^{-1} bands decreases and the ratio of 997~1030 cm^{-1} bands shows minor increase. That is to say, TiO_2 exists in the system mainly in the form of $[TiO_4]$ and the increase of TiO_2 leads to the increase of ratio of Q^0 structure unit and $[TiO_4]$ structural groups, reduction of Q^2 structure group, disappearance of the O-Si-O deformation. And simultaneously, some TiO_2 enters into Si-O-Si network to form (Si,Ti) coupling of stretch vibrations in a sheet structure.

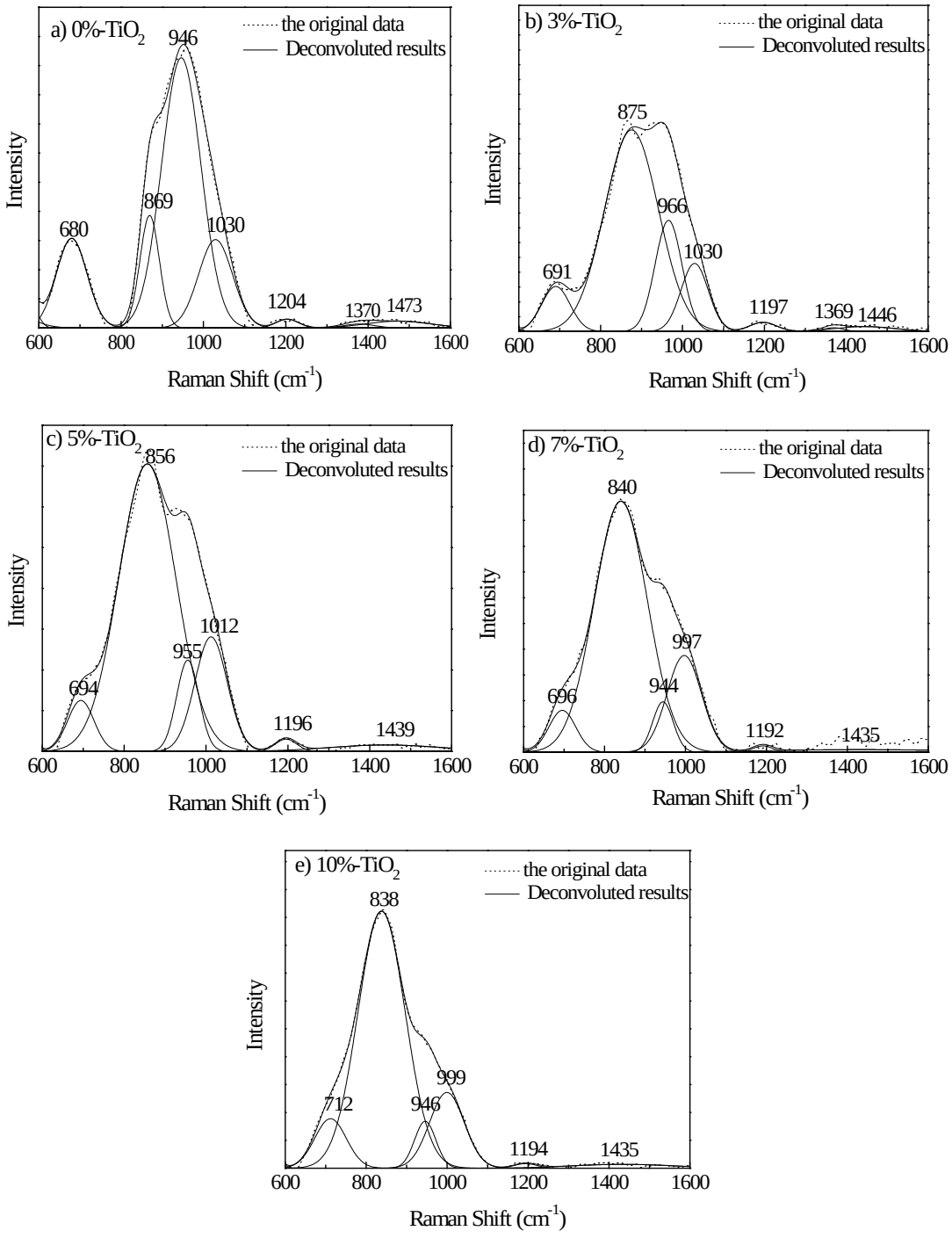

Fig. 5 Deconvoluted results of Raman spectra for samples with different TiO_2 contents

Besides, with increase of TiO_2, there appear a new band, 690~695 cm^{-1}, which shifts to 712 cm^{-1} as the content of TiO_2 increases to 10% in mass. According to Mysen et al [22], the band at approximately 690~695 cm^{-1} could be attributed to Ti-O stretch vibrations of Ti in six-fold coordination, [TiO_6], and the band at 720 cm^{-1} reflects the O-Ti-O deformation, so the band at 712 cm^{-1} could be proposed to the mixing of the [TiO_6] structure unit and O-Ti-O deformation. There are also some changes for bands in high frequency with the increase of TiO_2. It can be seen from Figure 6 that, the ratio of Raman bands for small borate structure group, pyroborate (1192~1204 cm^{-1}), has somewhat decrease and the ratio of Raman bands for large borate structure group (1369~1379, 1435~1470 cm^{-1}) decreases to a certain extent.

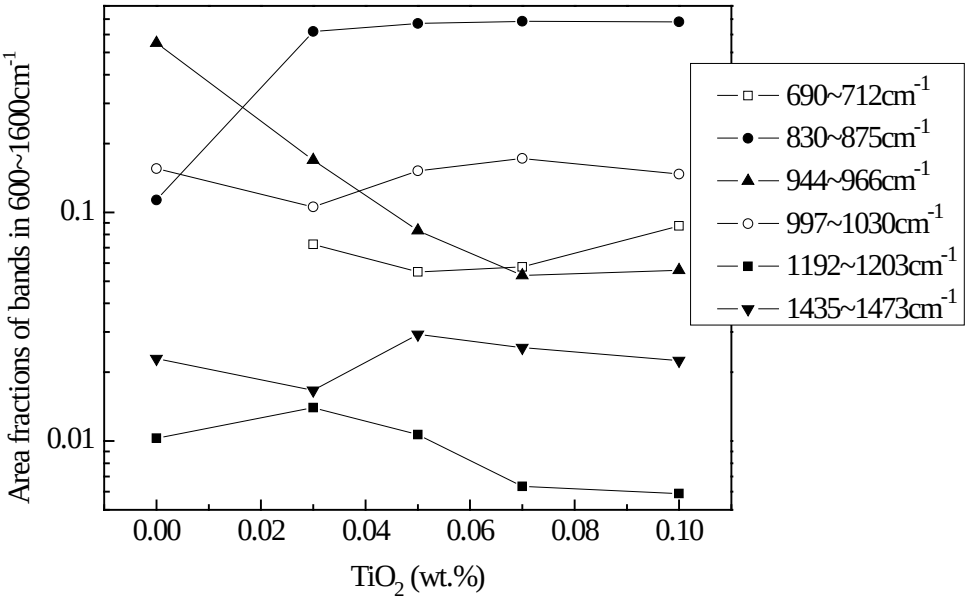

Fig. 6 Area fractions of bands in 600~1600 cm^{-1} as functions of TiO_2 contents

In general, it can be concluded that increasing the content of TiO_2 leads to the appearance of [TiO_4] and [TiO_6] structure groups and [TiO_4] becomes the main structure unit in the system; TiO_2 produces a certain destructive effect on Si-O-Si network structure as well as large borate group and conducive to the formation of some other complex structure groups, such as (Si,Ti) coupling in sheet unit.

The deconvoluted results of Raman spectra for glass samples with different B_2O_3 content are presented in Figure 7. In the glass system without B_2O_3 (Figure 7 (a)), the main structure units are mixing of the Q^0 structure unit and [TiO_4] structural groups, Q^2 in chain structure unit, [TiO_6] unit as well as mixing of (Si,Ti) coupling of stretch vibrations in a sheet structure and Si-O^o antisymmetric stretching in any structural units that contain bridging oxygen and. Figure 8 shows the area fractions of bands in 600~1600 cm^{-1} as functions of B_2O_3 contents. It can be observed that, as the content of B_2O_3 increases, the ratio of the dominant peak (in the vicinity of 866 cm^{-1}) decreases and the ratio of bands for sheet structure units (1010~1014 cm^{-1}) shows an increased tendency. It can be seen from Figure 7 and Figure 8 that as minor B_2O_3 is added into the system, such as 3% in mass, there firstly forms pyroborate structure unit, then, with the

increase of B_2O_3 content, BO_2O^- triangles units attached to the large borate group appear, and simultaneously the ratio of these borate structure groups increases to a certain extent. As the content of B_2O_3 reaches 10% in mass, the band at about 695 cm^{-1} move to the vicinity of 712 cm^{-1}, that is, there forms some amount of O-Ti-O deformation due to the increase of B_2O_3. By and large, existence of B_2O_3 leads to enhancement of polymerization degree of the slag system.

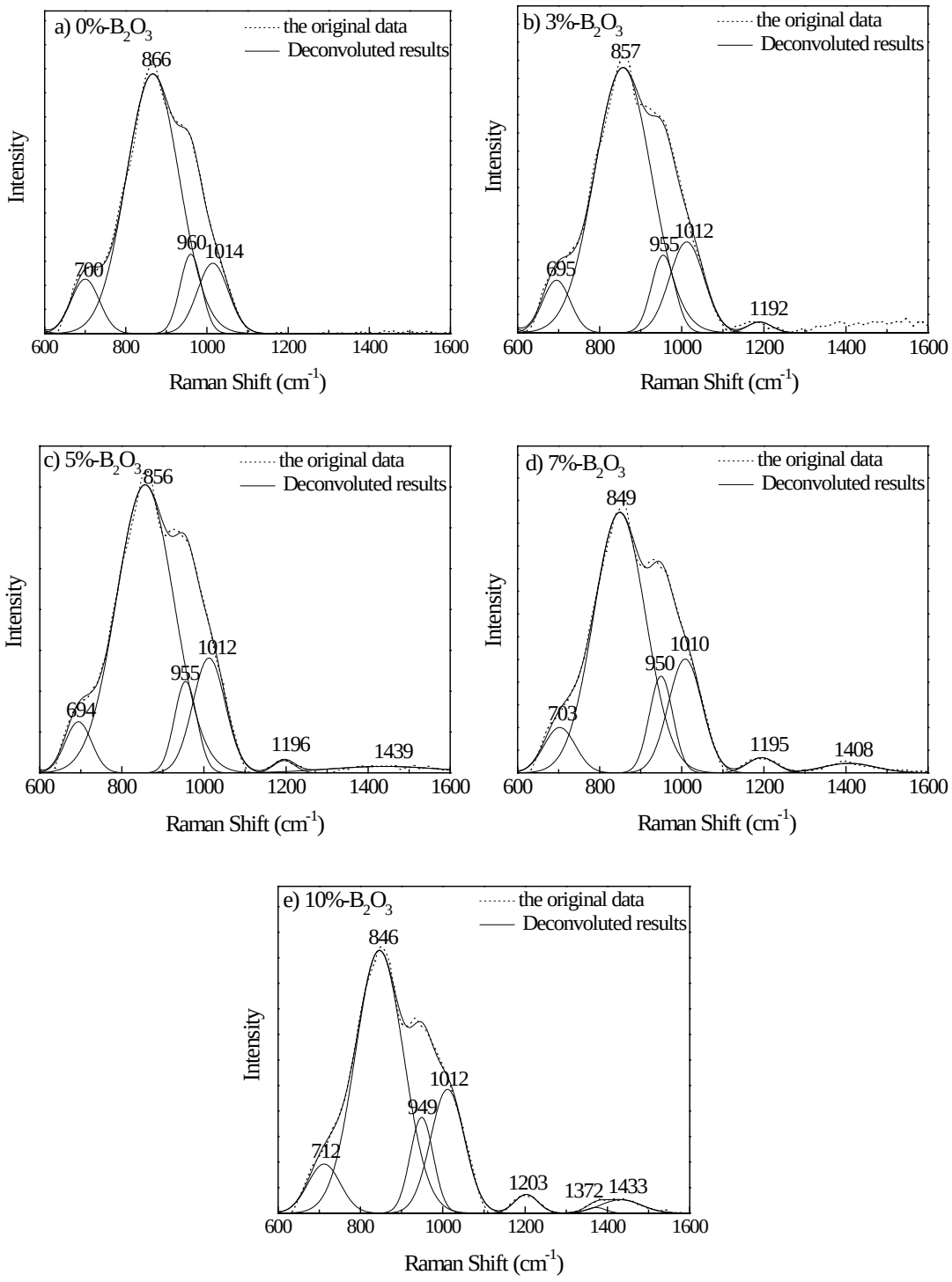

Fig. 7 Deconvoluted results of Raman spectra for glass samples with different B_2O_3 content

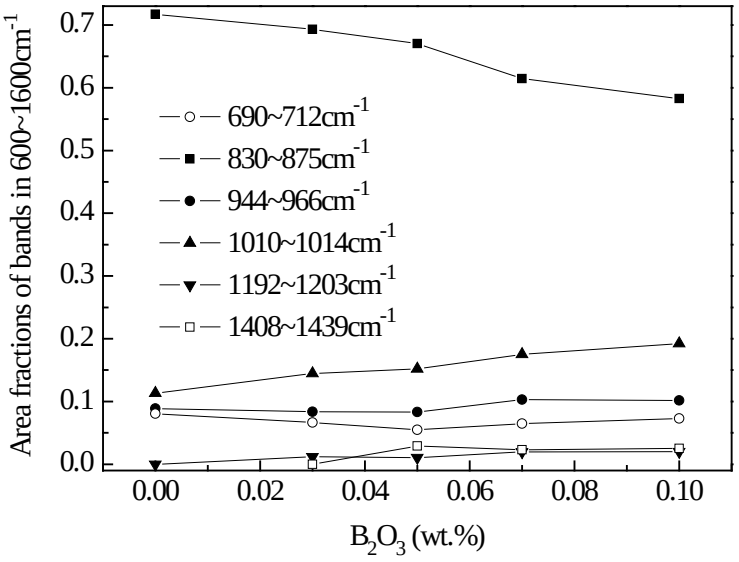

Fig. 8 Area fractions of bands in 600~1600 cm^{-1} as functions of B_2O_3 contents

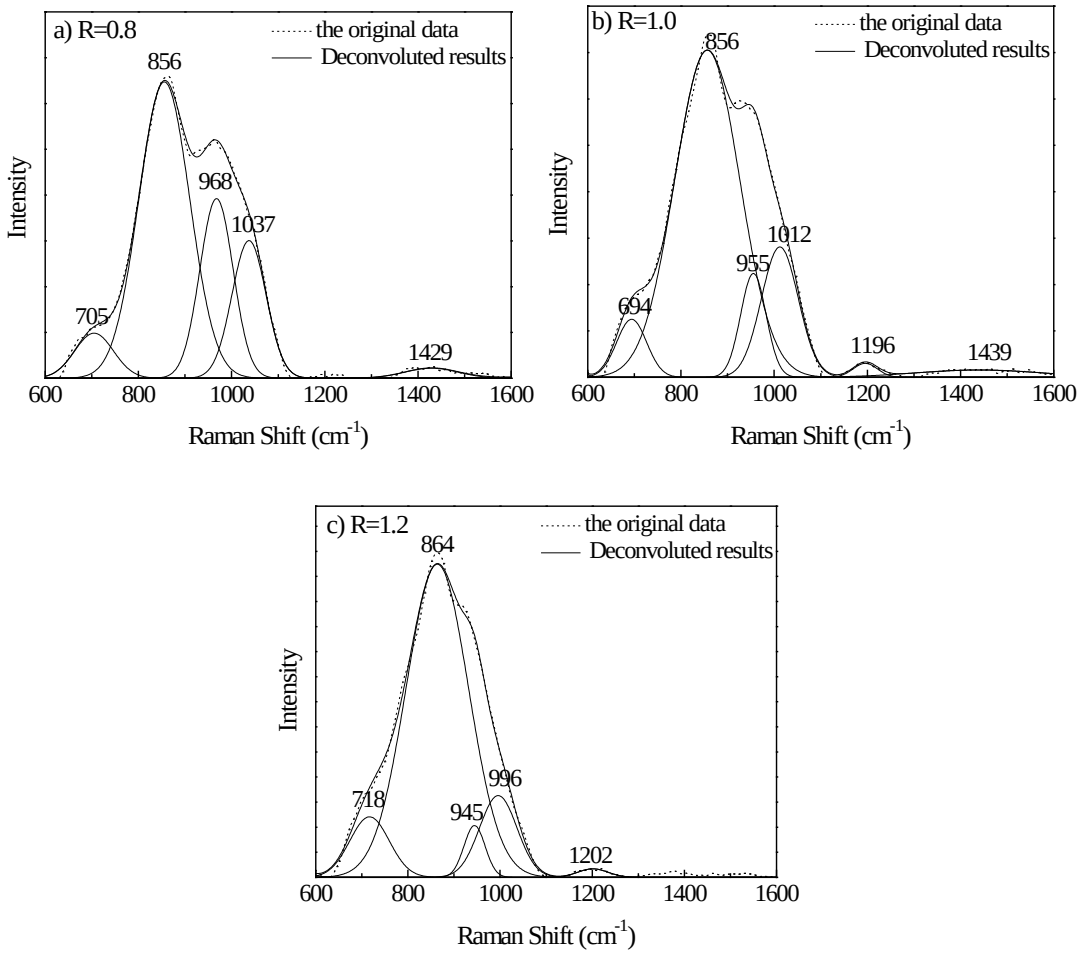

Fig. 9 Deconvoluted results of Raman spectra for glass samples with different basicities

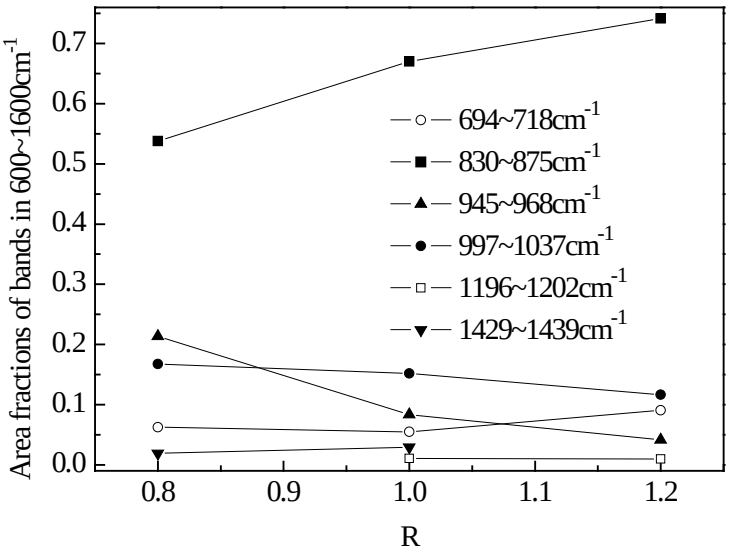

Fig. 10 Area fractions of bands in 600~1600 cm^{-1} as functions of basicities

Figure 9 exhibits the deconvoluted results of Raman spectra for glass systems with different basicities. It can be seen that, when the basicity is 0.8, the structure groups exist in the system mainly in the form of mixing of the Q^0 structure unit and [TiO_4] structural groups (856~864 cm^{-1}), Q^2 in chain structure unit (945~968 cm^{-1}), mixing of (Si,Ti) coupling of stretch vibrations in a sheet structure and Si-O^o antisymmetric stretching in any structural units that contain bridging oxygen (996~1037 cm^{-1}), and B_2O_3 exists in the system primarily in the form of BO_2O^- triangles units attached to the large borate group. Figure 10 presents the area fractions of bands in 600~1600 cm^{-1} as functions of basicities. It can be seen that, as the basicity increases, both the ratio of Q^2 in chain structure unit (945~968 cm^{-1}) and sheet structure unit (996~1037 cm^{-1}) decrease, while the ratio of mixing of the Q^0 structure unit and [TiO_4] structural groups (856~864 cm^{-1}) increases. It can be concluded that increasing the basicity produces a certain destructive effect on Si-O-Si network. Also, with the increase of basicity, and the band for BO_2O^- triangles units attached to the large borate group becomes too weak to be detected and along with the appearance of small borate group, pyroborate unit. That is, the increase of basicity causes simplification of borate network structure. Namely, the increase of basicity causes to negative effects on the borate network and Si-O-Si structure containing bridging oxygen.

4. Conclusions

The Raman spectroscopy technique has provided a deep insight into the structure of the B_2O_3 and TiO_2-bearing fluoride-Free mold flux glass system. The increase of TiO_2 leads to the appearance of [TiO_4], [TiO_6] and O-Ti-O deformation structure groups. And TiO_2 exists in the slag mainly in the form of [TiO_4]. TiO_2 weakens the Raman signals of Q^2, O-Si-O deformation and BO_2O^- triangles units linked to the large borate group, increases the ratio of mixing of the Q^0 structure unit and [TiO_4] structural groups. That is to say, TiO_2 produces a certain destructive effect on Si-O-Si network structure as well as large borate group and conducive to the formation of some other complex structure groups, such as (Si,Ti) coupling in sheet structure unit.

With the increase of B_2O_3, the ratio of mixing of the Q^0 structure unit and [TiO_4] structural group decreases and the ratio of sheet structure unit increase, and the peak for BO_2O^- unit attached to the large borate group shows an increase in intensity. Generally, existence of B_2O_3 leads to the enhancement of polymerization degree of the slag system.

With the increase of basicity, the ratio of Q^2 and sheet structure unit decrease, and the ratio of mixing of the Q^0 structure unit and [TiO_4] structural group increase. And BO_2O^- triangles units linked to the large borate group weaken, along with the appearance of pyroborate group. It suggests that the increase of basicity produces negative effects on the borate network and Si-O-Si structure containing bridging oxygen, and reduces the degree of polymerization of the system.

Acknowledgement

The financial support from NSFC (No. 50704002) is gratefully acknowledged.

References

[1] M. Hayashi, N. Nabeshima, H. Fukuyama, K. Nagata. Effect of fluorine on silicate network for CaO-CaF_2-SiO_2 and CaO-CaF_2-SiO_2-FeO_x glasses. ISIJ Int., 2002, 42 (4), p 352-358.

[2] Guanghua WEN, Seetharaman SRIDHAR, Ping TANG, Xin QI, Yongqing LIU. Development of fluoride-free mold powders for peritectic steel slab casting. ISIJ Int., 2007, 47 (8), p1117-1125.

[3] Li Gui-rong, Wang Hong-ming, Dai Qi-xun, Zhao Yu-tao, Li Jing-sheng. Physical properties and regulating mechanism of fluoride-free and harmless B_2O_3-containing mould flux. J. Iron Steel Res. Int., 2007, 14 (1), p25-28.

[4] Xin Qi, Guang-Hua Wen, Ping Tang. Investigation on heat transfer performance of fluoride-free and titanium-bearing mold fluxes. J. Non-Cryst. Solids, 2008, 354, p5444-5452.

[5] S. Choi, D. Lee, D. Shin, S. Choi, J. Cho, J. Park. Properties of F-free glass system as a mold flux: viscosity, thermal conductivity and crystallization behavior. J. Non-Cryst. Solids, 2004, 345-346, p157-160.

[6] A. B. Fox, K. C. Mills, D. Lever, C. Bezerra, C. Valadares, I. Unamuno, J. J. Laraudogoitia, J. Gisby. Development of Fluoride-Free Fluxes for Billet Casting. ISIJ Int., 2005, 45 (7), p1051-1058.

[7] H. Nakada, K. Nagata. Crystallization of CaO-SiO_2-TiO_2 slag as a candidate for fluorine free mold flux. ISIJ Int., 2006, 46 (3), p441-449.

[8] X.Qi, G. H. Wen, P. Tang. Viscosity and viscosity estimate model of fluoride-free and titanium-bearing mold fluxes. J. Iron Steel Res., Int., 2010, 17 (6), p06-10.

[9] K. C. Mills, A. B. Fox. The role of mould fluxes in continuous casting-so Simple yet so complex. ISIJ Int., 2003, 43 (10), p1479-1486.

[10] A. Grandjean, M. Malki, C. Simonnet, D. Manara, B. Penelon. Correlation between electrical conductivity, viscosity, and structure in borosilicate glass-forming melts. Phys. Rev. B, 2007, 75 (5), p054112-1- 054112-7.

[11] C. Gheorghies, I. Crudu, C. Teletin, C. Spanu. Theoretical model of steel continuous casting technology. J. Iron Steel Res. Int., 2009, 16 (1), p12-16.

[12] Andrzej Kudelski. Analytical applications of Raman spectroscopy. Talanta, 2008, 76 (1), p1-8.

[13] S. Kashio, Y. Iguchi, T. Goto. Raman spectroscopic study of the structure of silicate slag. Trans. ISIJ., 1980, 20 (4), p251-253.

[14] F. A. Seifert, B. O. Mysen, D. Virgo. Structural similarity of glasses and melts relevant to petrological processes. Geochim. Cosmochim. Acta, 1981, 45 (10), p1879-1884.

[15] B. O. Mysen, L. W. Finger, D. Virgo, F. A. Seifert. Curve-fitting of Raman spectra of silicate glasse. Am. Mineral., 1982, 67, p686-695.

[16] B. O. Mysen, D. Virgo, C. Scarfe. Relations between the anionic structure and viscosity of silicate melts—a Raman spectroscopic study. Am. Mineral., 1980, 65, p690-710.

[17] P. McMillan. A Raman spectroscopic study of glasses in the system CaO-MgO-SiO_2. Am. Mineral., 1984, 69, p645-659.

[18] P. McMillan. Structural studies of silicate glasses and melts-applications and limitations of Raman spectroscopy. Am. Mineral., 1984, 69, p622-644.

[19] J. D. Frantza, B. O. Mysen. Raman spectra and structure of BaO-SiO_2, SrO-SiO_2 and CaO-SiO_2 melts to 1600°C. Chem. Geol., 1995, 121, p155-176.

[20] B. O. Mysen, J. D. Frantza. Structure of silicate melts at high temperature: In-situ measurements in the system BaO-SiO_2 to 1669 ℃. Am. Mineral., 1993, 78, p699-709.

[21] B. O. Mysen, J. D. Frantz. Silicate melts at magmatic temperatures: in-situ structure determination to 1651 ℃ and effect of temperature and bulk composition on the mixing behavior of structural units. Contrib. Mineral. Petrol., 1994, 117, p1-14..

[22] B. O. Mysen, F. J. Ryerson, D. Virgo. The influence of TiO_2 on the structure and derivative properties of silicate melts. Am. Mineral., 1980, 65, p1150-1165.

[23] Z. N. Utegulov, J. P. Wicksted, G. Q. Shen. Role of Al formers and Na modifiers in Al_2O_3-SiO_2-Na_2O-MgO-Eu_2O_3 glassess: brillouin and Raman spectroscopy studies. Phys. Chem. Glasses, 2004, 45 (3), p166-172.

[24] B. O. Mysen, D. Virgo, F. A. Seifert. The structure of silicate melts: implications for chemical and physical properties of natural magma. Rev. Geophys., 1982, 20 (3), p353-383.

[25] Kohei Fukumia, Junji Hayakawaa, Toru Komiyama. Intensity of Raman band in silicate glasses. J. Non-Cryst. Solids, 1990, 119 (3), p297-302.

[26] P. F. McMillan, G. H. Wolf, B. T. Poe. Vibrational spectroscopy of silicate liquids and glasses. Chem. Geol., 1992, 96 (3-4), p351-366.

[27] B. O. Mysen, Daniel Neuville. Effect of temperature and TiO_2 content on the structure of $Na_2Si_2O_5$-$Na_2Ti_2O_5$ melts and glasses. Geochim. Cosmochim. Acta, 1995, 59 (2), P325-342.

[28] B. N. Meera, J. Ramakrishna. Raman spectral studies of borate glasses. J. Non-Cryst. Solids, 1993, 159 (1-2), p1-21.

[29] W. L. Konijnendijk, J. M. Stevels. The structure of borate glasses studied by Raman scattering. J. Non-Cryst.

Solids, 1975, 18 (3), p307-331.

[30] E. I. Kamitsos, M. A. Karakassides, G. D. Chryssikos. Structure of borate glasses I: Raman study of caesium, rubidium, and potassium borate glasses. Phys. Chem. glasses, 1989, 30 (6), p229-234.

[31] E. I. Kamitsos, M. A. Karakassides, G. D. Chryssikos. Vibrational spectra of magnesium-sodium-borate glasses 2. Raman and mid-infrared investigation of the network structure. J. Phys. Chem., 1987, 91 (5), p1073-1079.

[32] G. D. Chryssikos, E. I. Kamitsos, W. M. Risen Jr.. A Raman investigation of cadmium borate and borogermanate glasses. J. Non-Cryst. Solids, 1987, 93 (1), p155-168.

[33] G. Padmaja, P. Kistaiah. Infrared and Raman spectroscopic studies on alkali borate glasses: evidence of mixed alkali effect. J. Phys. Chem. A, 2009, 113, p2397-2404.